●「HCV 抗体陽性」で受診したらまずHCV RNA の有無を確認する.
● HCV RNA 陰性でも肝機能異常があれば原因を精査する.
● HCV RNA 陽性が判明したら次に肝炎の有無について調べる.

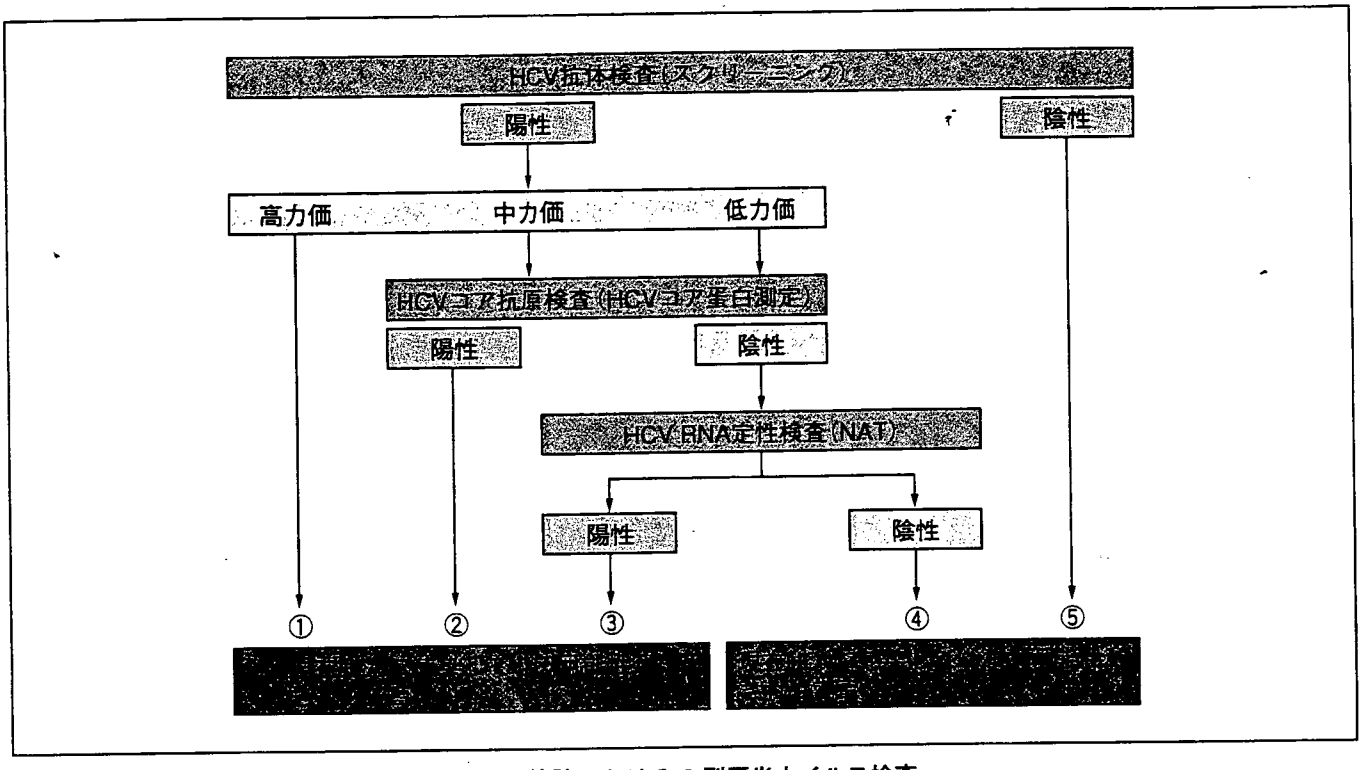

図1　検診におけるC型肝炎ウイルス検査
(文献2)より引用)

査とその判定手順は図1[2]に示す通りである．すなわち老人健康法に基づいた肝炎ウイルス検診を受けた場合はこの手順に沿って検査が行われており，いわゆるかかりつけ医などでHCV 抗体検査を受けたという場合と明確に区別されなければいけない．HCV 抗体検査だけの場合は低力価であれば既往感染の可能性も高いので，「HCV 抗体陽性を指摘された」といって受診があった場合はまずHCV 感染の有無を確認しなければならない．この場合には肝炎ウイルス検診等実施要綱と同様に，HCV 抗原検査を行った後にHCV 核酸増幅検査を行うか，すぐにHCV 核酸増幅検査を行うかは施設により異なるのが現状である．たとえHCV 感染が否定されても肝機能異常が存在すればアルコール性肝疾患や非アルコール性脂肪性肝疾患を念頭において精査を進めるべきである．これに対して肝炎ウイルス検診陽性者が受診した場合には文字通り「現在，C 型肝炎ウイルスに感染している可能性がきわめて高い」と判断される．

b.　肝炎の有無について

HCV 感染が確認されたら次に肝炎の有無，すなわちトランスアミナーゼが正常域か否かを判定する必要がある．近年，血清ALT 値の正常値について重要な論文[1]が報告されているが，わが国においてもALT 値の正常値は各施設の正常域とするのでなく，一般的に30 IU/*l* 以下と考えられている．すなわちALT 値が施設の正常域内であっても30 IU/*l* を超えている場合は軽度の肝炎が存在しうることを念頭におくべきである．また，たとえALT 値が30 IU/*l* 以下であっても1回の血液検査のみで無症候性キャリアと判断してはならない．C 型慢性肝疾患の場合は肝臓の線維

●肝炎の存在が疑われたら肝線維化の程度を評価する.
● HCV の場合は血小板数が肝線維化の評価に有用である.
●なぜC型肝炎に対する治療が必要であるかを自然経過と肝発癌の危険性から説明する.

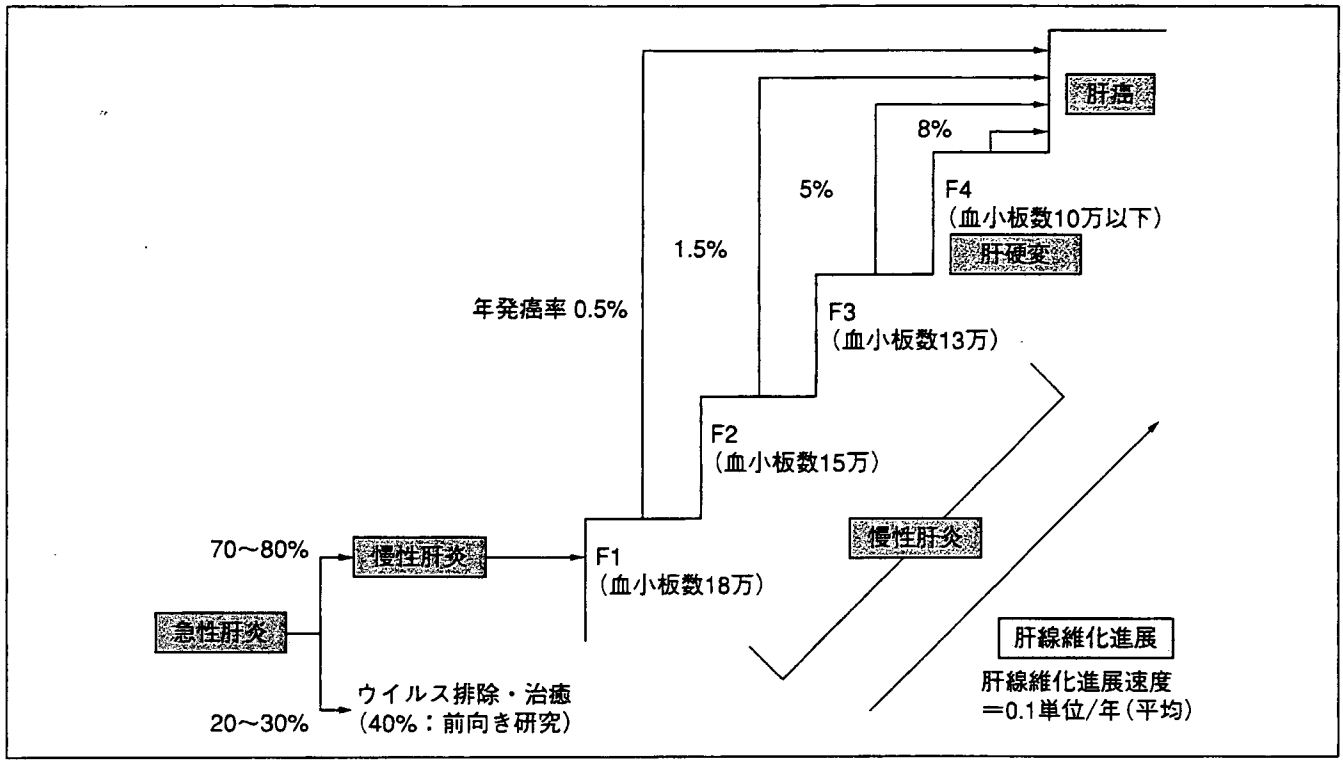

図2　C型肝炎の自然経過と肝癌への進展
(文献2)より引用)

化，すなわちstagingと血小板数との相関関係が認められることから血小板数の測定も合わせて行うべきである．腹部超音波検査による肝臓の形態を把握することは肝疾患の慢性度を評価するのに重要であり，血小板数と合わせて評価することでALT値が正常化しているような肝硬変の見落としもなくなってくる．肝生検から得られる情報は大きいが，stagingに関してはある程度血小板数とも相関し，最近では欧米を中心にfiroscanなどの非侵襲的方法により肝線維化を評価する傾向がひろがっている．肝組織検査の適応については基礎疾患の有無，必要性など多角的に検討して決定する必要がある．

c.　治療方針の決定

肝炎の存在が考えられれば治療を行う必要がある．C型慢性肝炎治療の第一選択はインターフェロン(IFN)(±リバビリン併用)療法であり，C型肝炎ウイルス感染者に対する治療の標準化に関する研究班(班長：熊田博光)の治療ガイドラインによれば遺伝子型とウイルス量の違いから治療方法が異なることから，ウイルスの遺伝子型と量の測定を行うべきである．この際に重要なことはC型慢性肝炎では自覚症状がないことがほとんどなので，なぜ治療を行う必要があるかを理解してもらうためにC型慢性肝炎の自然経過と肝発癌の危険性(図2)[2]について十分に説明することである．一方，先の治療ガイドラインによればALT値正常の無症候性キャリアに対しても血小板数を考慮した治療方針が記載されているが，これについては本特集号の別項に詳細に解説されているの

- HBs 抗原陽性者の場合もまず肝炎の有無を確認することが重要である.
- C 型慢性肝炎にくらべて B 型慢性肝炎では血小板と肝線維化の相関は弱い.
- B 型慢性肝炎では血清 ALT 値が低くても線維化が進行していることも多い.

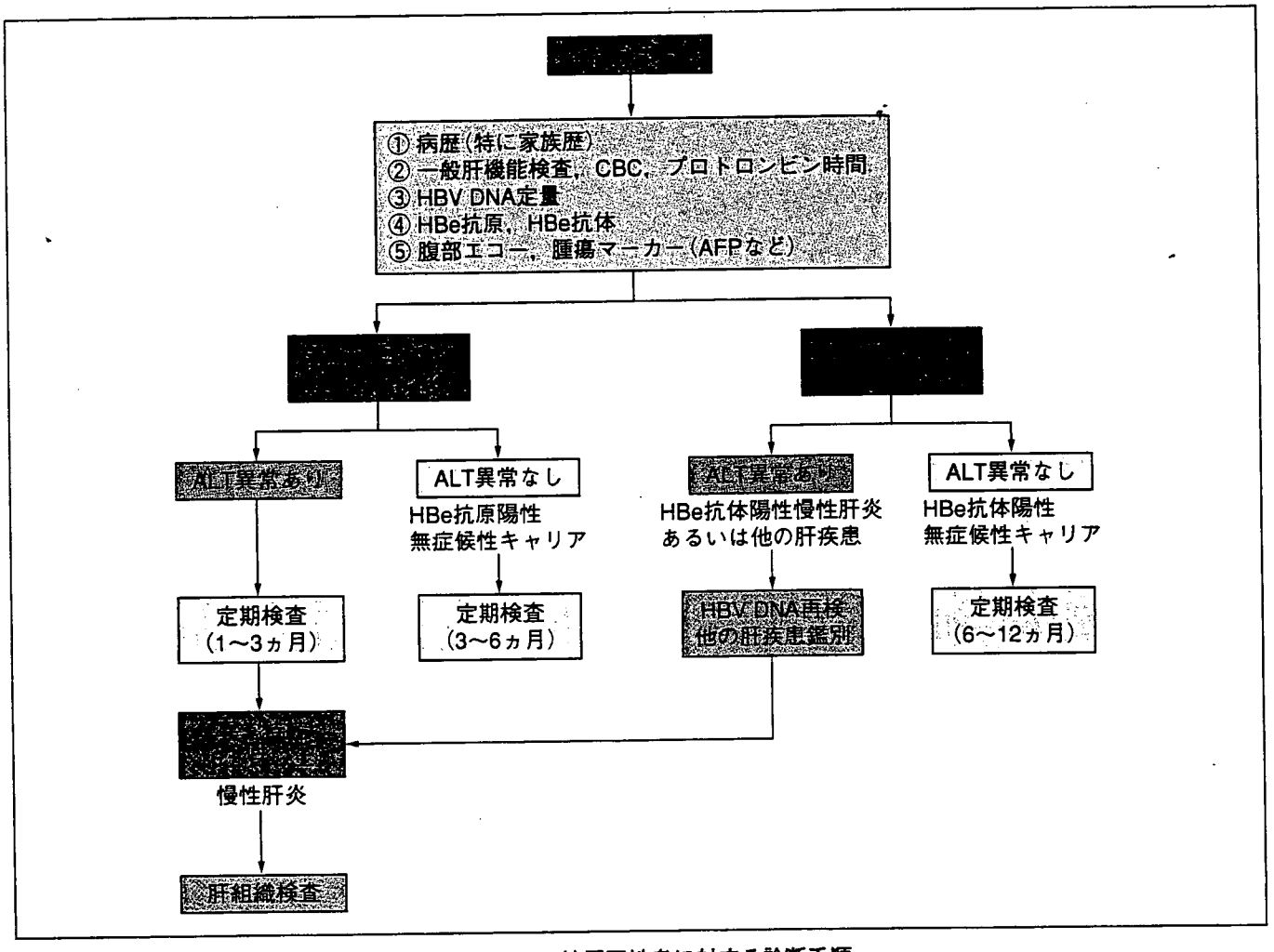

図 3　HBs 抗原陽性者に対する診断手順
(文献 2) より引用)

で省略する.

2. HBs 抗原陽性の場合

a. 診断と肝炎の有無について

急性肝炎でない限り肝炎ウイルス検診者が HBs 抗原陽性として受診した場合は HBV キャリアである. HBs 抗原陽性者に対する診断の手順については日本肝臓学会編集による「慢性肝炎の治療ガイド 2006」[2] によく書かれている(図 3). 肝炎の存在が疑われるときは，C 型慢性肝炎以上に肝組織診断(肝生検)が推奨される. これは B 型慢性肝疾患では血小板数と線維化の程度が C 型慢性肝炎ほどの相関を認めないことや，血清 ALT 値から予測される以上に炎症や線維化が進展していることが多いためである.

b. 治療方針の決定

HBV キャリアの診療では，患者が治療対象となるかどうかを決定することがきわめて重要である. HCV キャリアの場合は肝炎が存在すれば原則的に治療の適応があるが，HBV キャリアではたとえ HBV DNA 陽性や ALT 値の異常を認め

❸若年者のB型慢性肝炎では自然経過で肝炎が沈静化することも多い.
❹B型慢性肝炎の治療適応決定のために肝生検は重要である.
❺B型慢性肝炎の治療方針決定には肝臓専門医との相談も重要である.

ても，若年者ではしばしば自然経過の中でHBeセロコンバージョンし，肝炎の鎮静化を認めることを常に考慮すべきである．厚生労働省の班会議によるB型慢性肝炎の治療ガイドラインでも35歳を境に治療方針が異なっており，治療方針決定における年齢の重要性が示されている．当然のことながらHCVの場合と異なり，ウイルスの完全排除は不可能であるため，治療の目標がウイルス増殖低下に伴う肝炎の鎮静化であることをよく理解してもらう必要がある．最終的治療目標は発癌阻止，生存期間の延長，QOLの改善などである．しかし，経過中に著明なALT値の上昇を伴う急性増悪を経験することも多く，経過観察すべきか抗ウイルス療法あるいは肝庇護療法を行うべきか迷うことも少なくない．この場合に，“まだ待てる”すなわち経過観察しうるか否かの重要な判断材料は肝組織診断である．C型慢性肝炎に比べるとたとえガイドラインを参考にしても治療方針に苦慮することも多く，症例に応じた個々の対応を求められることが多いのがB型慢性肝炎の特徴でもあり，肝臓専門医に相談することも重要な手段であることを認識していただきたい．

おわりに●

この4年間の肝炎ウイルス検診により新たな肝炎ウイルスキャリアが発見されたが，肝炎ウイルス感染者に対して適切な対応をとってこそ検診の価値が発揮されることになる．肝炎ウイルス検診陽性者が受診した際には，肝炎が存在するか否か，治療が必要か否かについて判断し説明を行うことが重要である．また，たとえ肝炎が存在しなくてもウイルス性肝炎の自然経過を説明することにより定期的な経過観察が必要であることを理解してもらうように努めるべきである．

文　献

1) Prati, D. et al.：Updated definitions of healthy ranges for serum alanine aminotransferase levels. Ann Intern Med 137：1-9, 2002
2) 日本肝臓学会編：慢性肝炎の治療ガイド2006, 文光堂

C型肝炎と鉄代謝

日野　啓輔　山口大学大学院医学系研究科基礎検査学分野
仁科　惣治　山口大学大学院医学系研究科消化器病態内科学

日本臨床内科医会会誌第22巻第4号　別刷
（平成19年12月10日　発行）

◆消化器系領域

C型肝炎と鉄代謝

日野　啓輔　山口大学大学院医学系研究科 基礎検査学分野
仁科　惣治　山口大学大学院医学系研究科 消化器病態内科学

C型慢性肝炎の治療として認可された瀉血療法の目的が除鉄であることは周知の事実ですが，ではなぜ除鉄が必要なほどC型慢性肝炎患者さんには体内の鉄が多いのか，またなぜ除鉄を行う必要があるのかについては不明のままです．本稿ではHCVの全遺伝子が組み込まれたマウス（HCVトランスジェニックマウス：HCV TgM）を使ったわれわれの研究を紹介して，この疑問にお答えしたいと思います．

2001年にhepcidinというペプチドホルモン(肝臓で生成)が発見され，hepcidinが十二指腸の鉄吸収ならびにマクロファージの鉄放出を抑制することが明らかにされました．HCV TgMではこのhepcidinが低下しており，このため血清鉄と肝内鉄濃度は上昇していました．

次にHCV TgMの肝細胞を用いて検討したところhepcidinの転写活性が低下しており，この原因はhepcidinの転写を調節する転写因子（C/EBPα)の活性低下によるものでした．さらにこの転写因子の活性低下はHCVタンパクによる活性酸素を介して増加したCHOPというタンパクにより引き起こされていることが明らかになりました（図)．

ただし，このモデルでは肝臓に炎症がないのでC型慢性肝炎患者ではより複雑なメカニズムが働いていると予想されます．しかし，hepcidinの低下があるといってもHCV TgMに認められる肝内鉄沈着は軽微であり，C型慢性肝炎患者ほどの鉄蓄積を認めません．

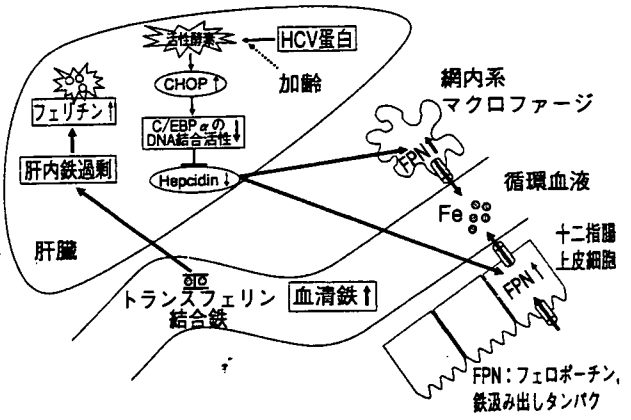

図　(Gastroenterology in press)

そこで鉄過剰が肝発癌にどのように関与するかを明らかにするために，通常餌の含有鉄の5倍濃度の鉄過剰餌をHCV TgMに与え，C型慢性肝炎患者とほぼ同等の肝内鉄濃度を有するHCV TgMを作成しました．

興味深いことに6ヵ月飼育すると小滴性脂肪を含む著明な肝内脂肪沈着を認め，ミトコンドリアの超微形態異常や機能異常(脂肪酸分解能の低下)が現われ，さらに12ヵ月になると肝臓内において脂質過酸化物の含有量が有意に上昇し，酸化的DNA傷害の指標である8-OHdGも有意に増加しました．

そして最も印象的なことは鉄過剰餌を与えたHCV TgMのみにHCCを含む肝腫瘍の発生(45%)を認めたことです．これら一連の成績についてはGastroenterology 2006；130：2087-98に報告していますのでご参照ください．

われわれはHCVが惹起する酸化ストレスや鉄代謝異常を切り口としてC型慢性肝疾患患者の肝発癌機構について研究していますが，本稿が先生方の知的好奇心を刺激し，日常診療においてもC型肝炎における鉄過剰の病的意義をご理解いただければこの上もない喜びです．

Liver International ISSN 1478-3223

BASIC STUDIES

Stronger Neo-Minophagen C™, a glycyrrhizin-containing preparation, protects liver against carbon tetrachloride-induced oxidative stress in transgenic mice expressing the hepatitis C virus polyprotein

Isao Hidaka[1], Keisuke Hino[2], Masaaki Korenaga[1], Toshikazu Gondo[3], Sohji Nishina[1], Miye Ando[2], Michiari Okuda[1] and Isao Sakaida[1]

1 Department of Gastroenterology and Hepatology, Yamaguchi University Graduate School of Medicine, Ube, Japan
2 Department of Basic Laboratory Sciences, Yamaguchi University Graduate School of Medicine, Ube, Japan
3 Department of Surgical Pathology, Yamaguchi University Hospital, Ube, Japan

Keywords
cytochrome P450 2E1 – γ-glutamylcysteine synthetase – glutathione – mitochondria

Correspondence
Keisuke Hino, MD, PhD, Department of Basic Laboratory Sciences, Yamaguchi University Graduate School of Medicine, 1-1-1 Minami-Kogushi, Ube, Yamaguchi 755-8505, Japan
Tel: +81 836 222 824
Fax: +81 836 222 824
e-mail: k.hino@yamaguchi-u.ac.jp

Received 10 January 2007
accepted 3 March 2007

DOI:10.1111/j.1478-3231.2007.01492.x

Abstract

Background/Aim: Stronger Neo-Minophagen C™ (SNMC), a glycyrrhizin-containing preparation, has been used as a treatment for chronic hepatitis for more than 30 years in Japan, and shown to be effective in preventing the development of hepatocellular carcinoma in chronic hepatitis C patients, but its underlying mechanisms remain elusive. The aim of this study was to investigate if SNMC had an anti-oxidative effect, as oxidative stress has been proposed to be one of the mechanisms of liver injury in hepatitis C virus (HCV)-associated chronic liver diseases. *Methods:* The protective effect of SNMC against carbon tetrachloride (CCl_4)-induced liver injury was examined using transgenic mice expressing the HCV polyprotein. *Results:* A small dose of CCl_4 (10 μl/kg of body weight) significantly increased the serum alanine aminotransferase (ALT) level and hepatic malondialdehyde content, decreased hepatic reduced glutathione (GSH) content and induced ultrastructural alterations of hepatic mitochondria in transgenic mice, but not in nontransgenic mice. A single SNMC treatment equivalent to a clinical dose significantly restored the serum ALT level and hepatic malondialdehyde and GSH contents, attenuated the ultrastructural alterations of hepatic mitochondria, and increased mRNA expression of γ-glutamylcysteine synthetase (γ-GCS). *Conclusions:* Transgenic mice expressing the HCV polyprotein are abnormally vulnerable to oxidative stress. SNMC protects hepatocytes against CCl_4-induced oxidative stress and mitochondrial injury in the presence of HCV proteins by restoring depleted cellular GSH.

Chronic hepatitis C virus (HCV) infection is associated with progressive liver disease that may evolve insidiously to cirrhosis with an increased risk of hepatocellular carcinoma (HCC) and liver failure (1–3). Antiviral treatment with (peg)interferon–ribavirin combination therapy has been successful in 50–85% of patients over the past decade (4, 5). For those not responding or those patients with absolute contraindications to this combination therapy, different treatment strategies are needed. Studies on chronic hepatitis B and C have shown that persistent normalization of alanine aminotransferase (ALT) is important in reducing the complications of chronic hepatitis including development of HCC, regardless of ongoing viral replication (6, 7).

In Japan, a glycyrrhizin-containing preparation, Stronger Neo-Minophagen C™ (SNMC), has been used as a treatment for chronic hepatitis for more than 30 years. It is available in an injectable form for intravenous administration, containing 0.2% glycyrrhizin, 0.1% L-cystein and 2.0% glycine in physiologic solution. Glycyrrhizin is an aqueous extract of licorice root (*Glycyrrhizae radix*), which has anti-allergic, anti-inflammatory and detoxicating effects (8). The anti-

inflammatory mechanism of SNMC is thought to be owing to its protective effect on the hepatic cellular membrane (9, 10). In a double-blind randomized placebo-controlled trial, Suzuki et al. (11) reported that in Japanese patients with chronic hepatitis, serum transaminases decreased during the treatment with SNMC. A recent European randomized trial also showed biochemical and histological effects of 26-week treatment with SNMC in patients with chronic hepatitis C (12). In addition, Arase et al. (13) demonstrated that long-term usage of SNMC was effective in preventing HCC development in Japanese patients with chronic hepatitis C. However, that study was retrospective and the mechanisms by which SNMC prevents HCC development remain elusive.

Oxidative stress has been proposed to be one of the mechanisms of liver injury in HCV-associated chronic liver diseases (14–17) and increased markers of oxidative stress are a well-known feature (18–20). Oxidative stress favours DNA damage, genetic instability and tumorigenesis. Indeed, we have reported that HCV transgenic mice fed an excess iron diet show marked steatosis and mitochondrial injury at 6 months, and an increase in the hepatic content of lipid peroxidation products and 8-hydroxy-2′-deoxyguanosine and subsequent development of HCC at 12 months after the initiation of feeding (21). This animal model, therefore, seemed to be useful for studying the mechanisms by which the long-term treatment with SNMC prevents HCC development in persistent HCV infection. In addition, we chose to use carbon tetrachloride (CCl_4) to induce mild oxidative stress in transgenic mice, since we previously observed that a low dose of CCl_4 caused the liver damage with oxidative stress in other HCV transgenic mice (16). The aim of this study was to ascertain if SNMC had a protective effect against the liver damage with oxidative stress, which would provide us with a rationale for conducting long-term treatment with SNMC in HCV transgenic mice.

Materials and methods

Animals

The transgene pAlbSVPA-HCV, containing the full-length polyprotein-coding region (core to NS5B, nts 342-9378) of genotype 1b, of the HCV-N strain of HCV (22), under the control of the murine albumin promoter/enhancer, was described in detail by Lerat et al. (23). Of the four transgenic lineages with evidence of ribonucleic acid (RNA) transcription of the full-length HCV-N open reading frame (FL-N), the FL-N/35 lineage proved capable of breeding in large numbers. There was no inflammation in transgenic livers (23). Transgenic animals were mated with normal C57BL/6 mice to produce subsequent-generation animals. These subsequent-generation animals were identified by polymerase chain reaction (PCR) analysis, as described previously (21). FL-N/35 transgenic mice and age-matched C57BL/6 mice were bred and maintained according to the criteria outlined in the 'Guide for the Care and Use of Laboratory Animals'.

Experimental design

FL-N/35 transgenic male mice and their normal C57BL/6 male littermates (nontransgenic mice) aged 3 months were injected intraperitoneally with 10 μl/kg of body weight CCl_4 (Wako Pure Chemical, Osaka, Japan) in corn oil with/without subsequent subcutaneous injection of 50 μl of SNMC (supplied by Minophagen Pharmaceutical Co. Ltd, Tokyo, Japan) 30 min after CCl_4 injection: nontransgenic mice were injected with CCl_4, FL-N/35 transgenic mice with CCl_4, nontransgenic mice with CCl_4 followed by SNMC and FL-N/35 transgenic mice with CCl_4 followed by SNMC. SNMC consists of 40 mg of glycyrrhizin, 20 mg L-cystein and 400 mg of glycine in 20 ml of physiological saline. Untreated animals were used as controls. Four to six mice in each group were killed by intraperitoneal injection of 10% pentobarbital sodium at 12 or 24 h after CCl_4 injection, and blood samples and liver tissue were collected for determination of the serum ALT level, hepatic content of lipid peroxidation products, cytochrome P450 2E1 (CYP2E1), reduced glutathione (GSH) and γ-glutamylcysteine synthetase (γ-GCS) and histology.

Hepatic lipid peroxidation-derived adducts

Resected fresh liver tissues were weighed and homogenized with saline. Homogenates were assayed for lipid peroxidation products. Malondialdehyde (MDA), one of aldehydic metabolites of lipid peroxidation, was quantified by the method of Yagi (24), by using a WAKO lipid peroxidation-test (Wako Pure Chemical). Hepatic MDA content was expressed as nanomoles per gram of liver weight.

Histological procedures

A portion of liver tissue was immediately snap frozen in liquid nitrogen for RNA extraction, protein extraction and determination of the hepatic GSH level. The remaining liver tissue was fixed in 4% paraformaldehyde in phosphate-buffered saline and embedded in paraffin for histological analysis. Liver sections were

stained with H&E and Masson's trichrome method for fibrosis.

Electron microscopy

Liver specimens were fixed in 2.1% glutaraldehyde, postfixed in 1% osmium tetroxide, dehydrated in graded ethanol and propylene dioxide, and embedded in Epok. Thin sections were stained with uranyl acetate and lead citrate and examined using a Hitachi-7000 transmission electron microscope (Hitachi Ltd, Tokyo, Japan).

Immunoblotting of cytochrome P450 2E1 (CYP2E1)

Resected liver tissues were homogenized in cell lysis buffer (Daiichi-Kagaku, Tokyo, Japan), containing 10 μl/ml of protease inhibitor cocktail (Sigma, St Louis, MO, USA) and 1 mM phenylmethylsulphonyl fluoride (Roche Molecular Biochemicals, Tokyo, Japan). Protein samples (20 μg of protein) were separated by sodium dodecyl sulphate-polyacrylamide gel electrophoresis on a 10–20% gel. The proteins were electrophoretically transferred to polyvinylidene difluoride membranes (Millipore, Bedford, MA, USA), blocked overnight at 4 °C with 5% skimmed milk and 0.1% Tween 20 in Tris-buffered saline and subsequently incubated for 1 h at room temperature with a goat polyclonal anti-rat CYP2E1 antibody (1:3000; Daiichi-Kagaku, Tokyo, Japan). This anti-rat antibody has been shown to work in mice (25). The membranes were washed, incubated with appropriate secondary antibodies and detected with ECLTM Western blot detection reagents (Amersham Biosciences, Piscataway, NJ, USA).

Hepatic content of GSH

Fifty milligrams of liver tissues was minced and sonicated in ice-cold 5% trichloroacetic acid and centrifuged at 3000g at 4 °C for 10 min. GSH content in the liver was measured by the thioester method, using a GSH-400 kit (OXIS International Inc., Portland, OR, USA). Protein concentrations in liver were determined by the method of Bradford et al. (26), by using the Quick start Bradford™ Dye Reagent (Bio-Rad Laboratories Inc., Hercules, CA, USA). Hepatic GSH content was expressed as nanomole per milligram of protein in the liver.

Messenger RNA expression (mRNA) of γ-glutamylcysteine synthetase (γ-GCS)

Total RNA was extracted from the frozen liver tissues using an RNeasy mini kit (Qiagen, Hilden, Germany). One-step real-time reverse transcription (RT)-PCR was performed with a Light Cycler using a QuantiTect SYBR Green RT-PCR Kit (Qiagen), according to the manufacturer's instructions. The melting-point analysis of all samples and controls was performed within the range from 65 to 95 °C. The primers amplifying the genes coding the heavy subunit (γ-GCS_H) and light subunit (γ-GCS_L) of γ-GCS are described in Table 1. The relative quantities of target mRNA used in the real-time RT-PCR were normalized with β-actin to compensate for variations in input RNA amounts.

Statistical analysis

Quantitative values are expressed as mean ± standard deviation. Two groups among multiple groups were compared by the rank-based, Kruskal–Wallis analysis of variance test followed by Scheffe's test because of non-homogeneity of variance among the groups. Data between two different groups were compared by the Mann–Whitney test. A P value of < 0.05 was considered to be significant.

Results

CCl_4-induced oxidative stress in FL-N/35 transgenic mice

Serum ALT levels remained normal in the basal condition in FL-N/35 transgenic and nontransgenic mice. FL-N/35 transgenic mice had significantly higher ALT levels in serum ($P < 0.0001$) at 24 h after intraperitoneal injection of CCl_4 as compared with those of the basal condition, but nontransgenic mice did not (Fig.

Table 1. Primers of the genes coding the heavy subunit (γ-GCS_H) and light subunit (γ-GCS_L) of γ-GCS

Genes	Sense	Antisense
γ-GCS_H	CTCCAGGTGACATTCCAAGCC[1]	GGCAGAAATCACTCCCCAGC[1]
γ-GCS_L	CACAATGACCCGAAAGAACTGCT[2]	GACTTGATGATTCCCCTGCTCTTC[2]
β-actin	TGACAGGATGCAGAAGGAGA[3]	GCTGGAAGGTGGACAGTGAG[3]

GenBank accession numbers are NM_010295 for 1, NM_008129 for 2, and NM_007393 for 3.
γ-GCS, γ-glutamylcysteine synthetase.

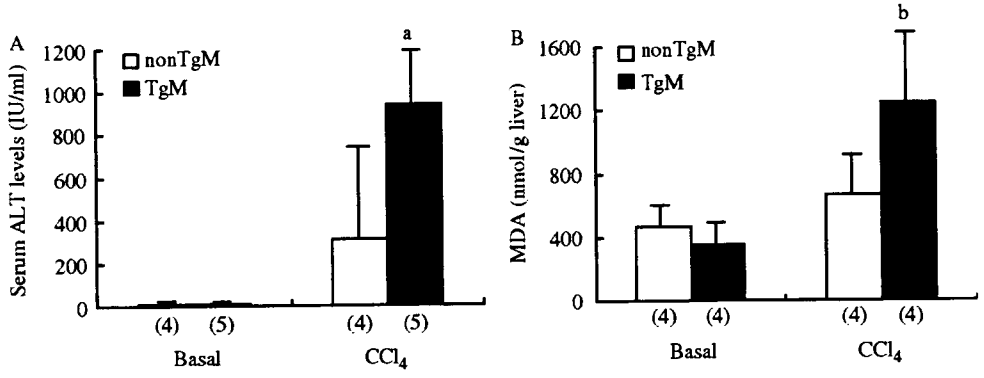

Fig. 1. Serum alanine aminotransferase (ALT) levels (A) and hepatic malondialdehyde (MDA) content (B) in FL-N/35 transgenic and nontransgenic mice in basal and carbon tetrachloride (CCl_4)-injected conditions. The numbers in parentheses represent the number of animals examined in each group. TgM, FL-N/35 transgenic mice; nonTgM, nontransgenic mice; a, $P < 0.0001$ vs TgM in basal condition; b, $P < 0.005$ vs TgM in basal condition.

1A). Similarly, there was no difference in hepatic MDA levels between FL-N/35 transgenic and nontransgenic mice in the basal condition. Intraperitoneal injection of CCl_4 significantly increased hepatic MDA levels after 24 h in FL-N/35 transgenic mice ($P = 0.005$), but not in nontransgenic mice (Fig. 1B). Nontransgenic mice did not show any significant histological changes such as inflammatory cell infiltration or hepatocytic degeneration at 24 h after CCl_4 injection. Liver histology of FL-N/35 transgenic mice after CCl_4 injection showed no infiltration of inflammatory cells, but swelling of hepatocytes in the perivenular zone (zone III) and mild steatosis, including the microvesicular type in the perivenular region and mid-zone (zone II) (Fig. 2A–D). The swollen hepatocytes seemed to contain vacuoles when observed at × 400 magnification. Thus, the small dose of CCl_4 used in the present study caused oxidative stress in FL-N/35 transgenic mice, but not in nontransgenic mice, which implied that FL-N/35 transgenic mice were more sensitive to oxidative stress than nontransgenic mice.

Protective effect of SNMC against CCl_4-induced oxidative stress in FL-N/35 transgenic mice

The CCl_4-induced significant increase in serum ALT levels was almost completely reversed by subcutaneous injection of 50 µl of SNMC 30 min after CCl_4 treatment in FL-N/35 transgenic mice ($P = 0.0009$) (Fig. 3A). SNMC treatment also restored the CCl_4-induced significantly increased MDA level in the liver to the basal level or reduced below it in FL-N/35 transgenic mice ($P = 0.0006$) (Fig. 3B). We next examined the hepatic content of GSH in FL-N/35 transgenic mice, since SNMC improved the liver injury induced by CCl_4. Although serum ALT levels and hepatic MDA levels significantly increased at 24 h after intraperitoneal injection of CCl_4, hepatic content of GSH was comparable with the basal level at this time point. However, the hepatic content of GSH significantly decreased at 12 h after CCl_4 injection in FL-N/35 transgenic mice as compared with the basal level ($P < 0.05$) (Fig. 3C). These results suggested that the hepatic GSH level was potentially restored by 24 h after CCl_4 administration. The depleted hepatic GSH content at 12 h after CCl_4 injection was restored by the treatment with SNMC in FL-N/35 transgenic mice ($P = 0.005$) (Fig. 3C). The swollen hepatocytes were absent and steatosis was less frequent in the liver in FL-N/35 transgenic mice treated with SNMC after CCl_4 injection (Fig. 2C–F). Thus, SNMC improved the liver injury induced by CCl_4 in FL-N/35 transgenic mice.

Hepatic expression of CYP2E1

Metabolism of CCl_4 begins with the formation of the trichloromethyl free radicals through the action of the cytochrome P450 oxygenase system of the endoplasmic reticulum (27). The major cytochrome isozyme that executes biotransformation of CCl_4 is CYP2E1. We therefore examined the hepatic expression of CYP2E1 in FL-N/35 transgenic mice on the assumption that SNMC may prevent the CCl_4-induced increase in CYP2E1 expression. However, CCl_4 injection did not increase the hepatic expression of CYP2E1 nor did SNMC change the hepatic expression of CYP2E1 at 12 and 24 h after CCl_4 injection (Fig. 4).

Ultrastructural alterations of mitochondria

As treatment with SNMC attenuated the CCl_4-induced swelling of hepatocytes and steatosis including

Liver International (2007)

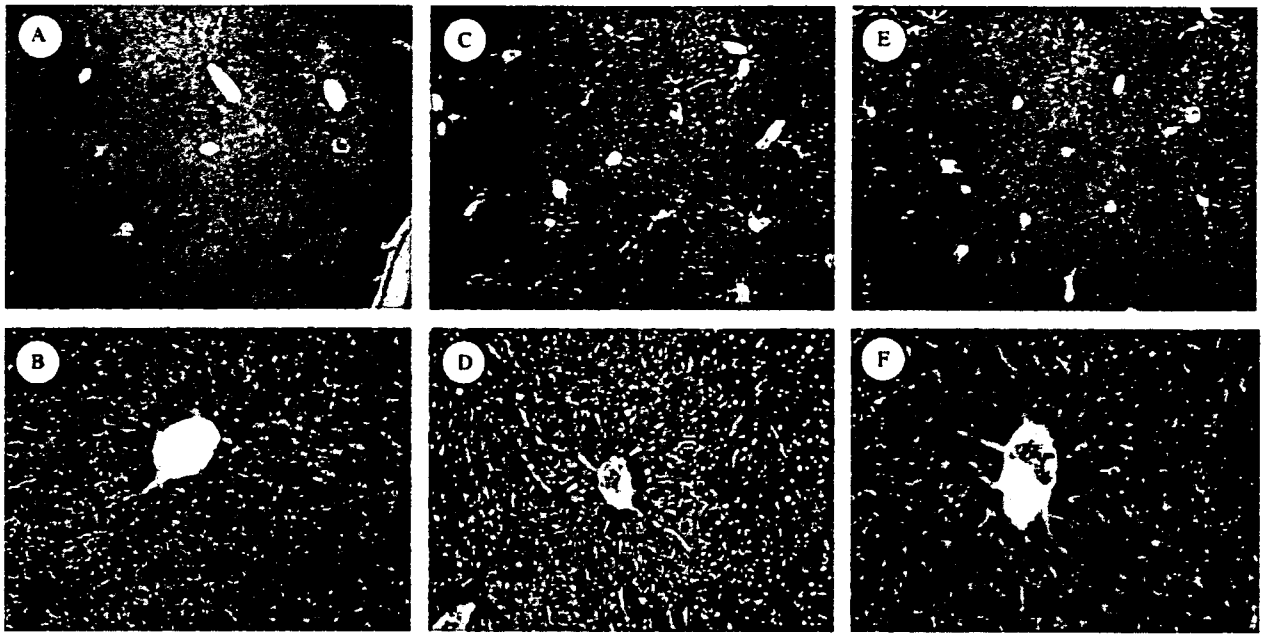

Fig. 2. Liver histology of FL-N/35 transgenic mice in basal (A and B) and carbon tetrachloride (CCl_4)- (C and D) or CCl_4 plus Stronger Neo-Minophagen C™ (SNMC)-injected conditions (E and F) (H&E, original magnification × 100 for A, C and E, × 400 for B, D and F). Liver histology of FL-N/35 transgenic mice after CCl_4 injection shows swelling of hepatocytes in the perivenular zone and mild steatosis including the microvesicular type, in the perivenular region and midzone. Such hepatocytic swelling was absent and steatosis was less frequent in the liver in FL-N/35 transgenic mice treated with SNMC after CCl_4 injection.

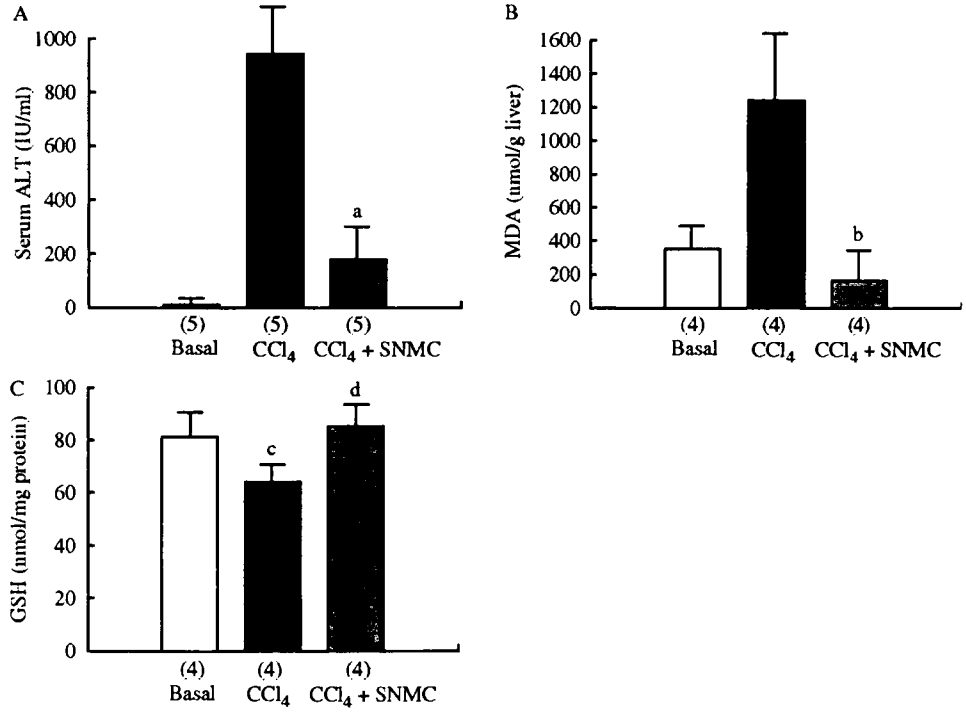

Fig. 3. Serum alanine aminotransferase (ALT) levels (A), hepatic malondialdehyde (MDA) content (B) and hepatic glutathione (GSH) content (C) in FL-N/35 transgenic mice in basal, carbon tetrachloride (CCl_4)- or CCl_4 plus Stronger Neo-Minophagen C™ (SNMC)-injected conditions. The numbers in parentheses represent the number of animals examined in each group. a, $P = 0.0009$ vs mice with CCl_4; b, $P = 0.0006$ vs mice with CCl_4; c, $P = .01$ vs mice in the basal condition; d, $P = 0.005$ vs mice with CCl_4.

the microvesicular type, we next examined the ultrastructure of the hepatocytic mitochondria in FL-N/35 transgenic mice. Even a modest dose of CCl_4 caused swelling of mitochondria in FL-N/35 transgenic mice. Such swollen mitochondria or irregular-sized mitochondria were less frequently found in FL-N/35 transgenic mice treated with SNMC after CCl_4 injection than in those without SNMC treatment (Fig. 5). Thus, SNMC attenuated the ultrastructural alterations of mitochondria induced by CCl_4 injection in FL-N/35 transgenic mice, suggesting that SNMC potentially protects mitochondria against oxidative stress.

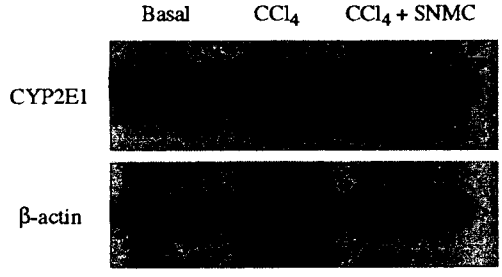

Fig. 4. Hepatic expression of CYP2E1 in FL-N/35 transgenic mice at 12 h after carbon tetrachloride (CCl_4) injection. Immunoblots for CYP2E1 were performed on liver lysates obtained from four mice in each group at 12 and 24 h after CCl_4 injection. CCl_4 injection did not increase the hepatic expression of CYP2E1 nor did Stronger Neo-Minophagen C™ (SNMC) change the hepatic expression of CYP2E1 at both time points.

mRNA expression of γ-GCS

γ-GCS is a heterodimer composed of γ-GCS_H and γ-GCS_L that associates, through disulphide binding, to form the holoenzyme (28, 29). We examined the mRNA expression of both subunits of γ-GCS at 12 h after CCl_4 injection in FL-N/35 transgenic mice, since SNMC-induced recovery from depletion of hepatic GSH was found at this time. In parallel with GSH, the expression of γ-GCS_L was significantly increased by the treatment with SNMC after CCl_4 injection ($P < 0.05$) (Fig. 6).

Discussion

Oxidative stress has been proposed to be one of the mechanisms of liver injury in HCV-associated chronic liver diseases (14–17) and increased markers of oxidative stress are a well-known feature in them (18–20).

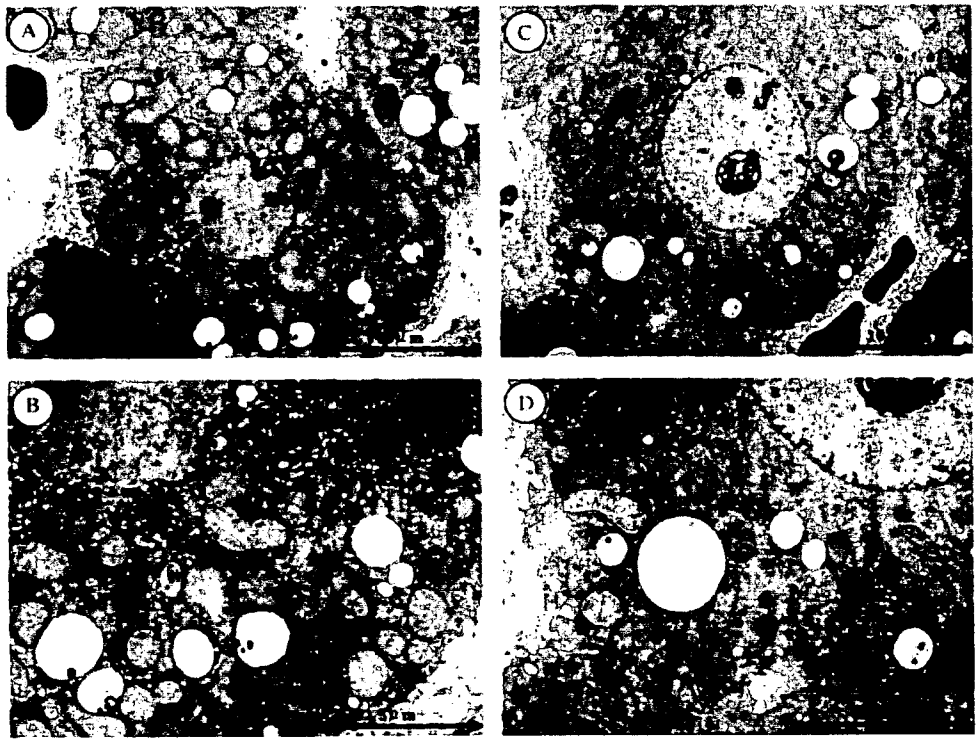

Fig. 5. Electron microscopy of the livers of FL-N/35 transgenic mice after carbon tetrachloride (CCl_4) injection (A and B) and CCl_4 plus Stronger Neo-Minophagen C™ (SNMC) injection (C and D). Swollen or irregular-sized mitochondria were less frequently found in FL-N/35 transgenic mice treated with SNMC after CCl_4 injection than in those without SNMC treatment (original magnification × 2000 for A and C, × 5000 for B and D).

Liver International (2007)

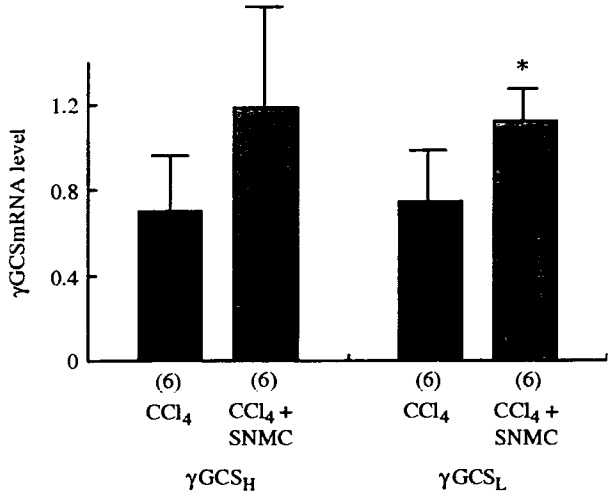

Fig. 6. Hepatic γ-glutamylcysteine synthetase (γ-GCS) mRNA levels in FL-N/35 transgenic mice at 12 h after injection of carbon tetrachloride (CCl_4) alone or CCl_4 plus Stronger Neo-Minophagen C™ (SNMC). The numbers in parentheses represent the number of animals examined in each group. *$P < 0.05$ vs mice with CCl_4.

However, the magnitude of oxidative stress induced by HCV proteins itself may not be large, as shown by the slow progression of liver disease in chronic hepatitis C patients with persistently normal aminotransferase levels. Clinical factors such as alcohol, iron overload and/or aging have been shown to reinforce the progression of liver disease in HCV infection (30–32). Oxidative stress induced by combination of HCV proteins with those factors is assumed to favour DNA damage, genetic instability and tumorigenesis. Long-term treatment with SNMC has been shown to be effective in preventing the development of HCC in patients with chronic hepatitis C (13). In this context, we wanted to know if SNMC had a protective effect against oxidative stress induced by the combination of HCV proteins with secondary stimulation, and examined this using transgenic mice expressing the HCV polyprotein. We chose to use CCl_4 to induce mild oxidative stress in transgenic mice. The type and extent of liver injury induced by CCl_4 cover a wide range of effects, depending on the dose and duration of exposure, or time of observation (33). The dose (10 μl/kg body weight) of CCl_4 used in this study was much less than those used for inducing oxidative stress in mice in previous studies (34–36), as we aimed to induce mild oxidative stress that was comparable with the clinical one observed in patients with chronic hepatitis C. This may explain why the expression of CYP2E1 was not significantly increased after CCl_4 treatment in FL-N/35 transgenic mice, even though CYP2E1 plays a central role in metabolizing CCl_4 (33). It should be noted that even such a small dose of CCl_4 induced a significant increase in serum ALT and hepatic MDA levels, and histological changes in FL-N/35 transgenic mice, though not in nontransgenic mice. These results show that FL-N/35 transgenic mice are abnormally vulnerable to oxidative stress. This observation is consistent with our previous observation that oxidative stress was significantly intensified by modest iron supplementation in FL-N/35 transgenic mice, but not in nontransgenic mice (21). Mitochondria are one of the main subcellular structures of hepatocytes affected by CCl_4 exposure (33). Even modest CCl_4 administration, which did not increase the expression of CYP2E1, caused ultrastructural alterations of hepatocytic mitochondria in FL-N/35 transgenic mice. In this context mitochondrial electron transport has been shown to be responsible for the free-radical activation by CCl_4 without the influence of CYP2E1 (37). We also reported that HCV core protein inhibits mitochondrial electron transport and increases reactive oxygen species production (17). Therefore, the small dose of CCl_4 may have reinforced the mitochondrial injury induced by HCV proteins. This may in part explain why FL-N/35 transgenic mice are abnormally vulnerable to oxidative stress. Thus, the CCl_4-induced mild oxidative stress observed in FL-N/35 transgenic mice seemed to be suitable for mimicking the oxidative stress induced by combination of HCV proteins with clinical factors such as alcohol, iron overload or aging in patients with HCV-associated chronic liver diseases.

The dose of SNMC administered to the FL-N/35 transgenic mice was comparable with the dosage given to patients with chronic hepatitis (approximately 100 ml of SNMC). This implies that a clinical dosage of SNMC is enough to reduce oxidative stress occurring in patients with HCV-associated chronic liver diseases. It should also be noted that SNMC treatment using a dose equivalent to a clinical dosage attenuated ultrastructural alterations of mitochondria induced by CCl_4. We previously reported the development of HCC preceded by marked hepatic steatosis, ultrastructural alterations of the mitochondria, decreased degradation activity of fatty acid and increases in the hepatic content of lipid peroxidation products in FL-N/35 transgenic mice fed an excess iron diet (21). In fact, we found that hepatic triglyceride content was significantly decreased by a 6-month treatment with SNMC in FL-N/35 transgenic mice fed the excess iron diet (I. Hidaka et al., unpublished observations). Therefore, SNMC appears to have the potential to prevent HCC development by reducing mitochondrial

injury induced by HCV and additional oxidative stress. Trichloromethyl free radicals derived from CCl_4 react with sulphthydyl groups such as GSH and protein thiols, and the covalent binding of trichloromethyl free radicals to the cell membrane is considered the initial step in a chain of events that eventually leads to membrane lipid peroxidation and finally to cell necrosis. It remains elusive whether GSH was primarily consumed against cytoplasmic oxidative tress or against mitochondrial oxidative stress or against both in the present model. Judging from the protective effect of SNMC against mitochondrial injury induced by CCl_4, inhibition of GSH depletion by SNMC may have contributed to reduction in mitochondrial oxidative stress in FL-N/35 transgenic mice. Hepatic GSH synthesis is mainly regulated by the availability of cysteine, the sulphur amino acid precursor, and the activity of the rate-limiting enzyme γ-GCS (38). SNMC consists of 0.2% glycyrrhizin, 0.1% cysteine and 2.0% glycine in physiologic solution. Originally SNMC was developed with the expectation of joint beneficial effects of the three components. The cysteine included in SNMC may have contributed to GSH synthesis through its increased availability. SNMC treatment also increased the synthesis of γ-GCS_L at the transcriptional level ($P < 0.05$). There are at least three possibilities that may account for this. First, glycyrrhizin may have activated γ-GCS at the transcriptional level. Second, cysteine may have activated γ-GCS as a substrate for γ-GCS. Third, both of the above may have worked together. The increase in γ-GCS_H expression by SNMC may have failed to reach a statistical significance ($P = 0.08$) owing to its greater deviation.

In conclusion, this study shows that transgenic mice expressing the HCV polyprotein are abnormally vulnerable to oxidative stress and that SNMC protects hepatocytes against CCl_4-induced oxidative stress in the presence of HCV proteins. SNMC also has protective effect against mitochondrial injury induced by CCl_4 in HCV transgenic mice.

References

1. Di Bisceglie AM, Goodman ZD, Ishak KG, Hoofnagle JH, Melpolder JJ, Alter HJ. Long-term clinical and histopathological follow-up of chronic posttransfusion hepatitis. *Hepatology* 1991; **14**: 969–74.
2. Tsukuma H, Hiyama T, Tanaka S, *et al.* Risk factors for hepatocellular carcinoma among patients with chronic liver disease. *N Engl J Med* 1993; **328**: 1797–801.
3. Tong MJ, el-Farra NS, Reikes AR, Co RL. Clinical outcomes after transfusion-associated hepatitis C. *N Engl J Med* 1995; **332**: 1463–6.
4. Manns MP, McHutchison JG, Gordon SC, *et al.* Peginterferon alfa-2b plus ribavirin compared with interferon alfa-2b plus ribavirin for initial treatment of chronic hepatitis C: a randomised trial. *Lancet* 2001; **358**: 958–65.
5. Fried MW, Shiffman ML, Reddy KR, *et al.* Peginterferon alfa-2a plus ribavirin for chronic hepatitis C virus infection. *N Engl J Med* 2002; **347**: 975–82.
6. Fattovich G, Giustina G, Degos F, *et al.* Effectiveness of interferon alfa on incidence of hepatocellular carcinoma and decompensation in cirrhosis type C. European concerted action on viral heaptitis (EUROHEP). *J Hepatol* 1997; **27**: 201–5.
7. Kasahara A, Hayashi N, Mochizuki K, *et al.* Risk factors for hepatocellular carcinoma and its incidence after interferon treatment in patients with chronic hepatitis C. Osaka liver disease study group. *Hepatology* 1998; **27**: 1394–402.
8. Finney RSH, Somers GF. The anti-inflammatory activity of glycyrrhetinic acid and derivatives. *J Pharm Pharmacol* 1958; **10**: 613–20.
9. Nakamura T, Fujii T, Ichihara A. Enzyme leakage due to change of membrane permeability of primary cultured rat hepatocytes treated with various hepatotoxins and its prevention by glycyrrhizin. *Cell Biol Toxicol* 1985; **1**: 285–95.
10. Shiki Y, Shirai K, Saito Y, Yoshida S, Mori Y, Wakashin M. Effect of glycyrrhizin on lysis of hepatocyte membranes induced by anti-liver cell membrane antibody. *J Gastroenterol Hepatol* 1992; **7**: 12–6.
11. Suzuki H, Ohta Y, Takino T, Fujisawa K, Hirayama C. Effects of glycyrrhizin on biochemical tests in patients with chronic hepatitis. *Asian Med J* 1983; **26**: 423–38.
12. Orlent H, Hansen BE, Willems M, *et al.* Biochemical and histological effects of 26 weeks of glycyrrhizin treatment in chronic hepatitis C: a randomized phase II trial. *J Hepatol* 2006; **45**: 539–46.
13. Arase Y, Ikeda K, Murashima N, *et al.* The long term efficacy of glycyrrhizin in chronic hepatitis C patients. *Cancer* 1997; **79**: 1494–500.
14. Barbaro G, Di Lorenzo G, Asti A, *et al.* Hepatocellular mitochondrial alterations in patients with chronic hepatitis C: ultrastructural and biochemical findings. *Am J Gastroenterol* 1999; **94**: 2198–205.
15. Valgimigli M, Valgimigli L, Trere D, *et al.* Oxidative stress EPR measurement in human liver by radical-probe technique. Correlation with etiology, histology and cell proliferation. *Free Radic Res* 2002; **36**: 939–48.
16. Okuda M, Li K, Beard MR, *et al.* Mitochondrial injury, oxidative stress, and antioxidant gene expression are induced by hepatitis C virus core protein. *Gastroenterology* 2002; **122**: 366–75.
17. Korenaga M, Wang T, Li Y, *et al.* Hepatitis C virus core protein inhibits mitochondrial electron transport and increases

reactive oxygen species (ROS) production. *J Biol Chem* 2005; **280**: 37481–8.
18. Jain SK, Pemberton PW, Smith A, *et al.* Oxidative stress in chronic hepatitis C: not just a feature of late stage disease. *J Hepatol* 2002; **36**: 805–11.
19. Paradis V, Mathurin P, Kollinger M, *et al.* In situ detection of lipid peroxidation in chronic hepatitis C: correlation with pathological features. *J Clin Pathol* 1997; **50**: 401–6.
20. Kitase A, Hino K, Furutani T, *et al.* In situ detection of oxidized n-3 polyunsaturated fatty acids in chronic hepatitis C: correlation with hepatic steatosis. *J Gastroenterol* 2005; **40**: 617–24.
21. Furutani T, Hino K, Okuda M, *et al.* Hepatic iron overload induces hepatocellular carcinoma in transgenic mice expressing the hepatitis C virus polyprotein. *Gastroenterology* 2006; **130**: 2087–98.
22. Beard MR, Abell G, Honda M, *et al.* An infectious molecular clone of a Japanese genotype 1b hepatitis C virus. *Hepatology* 1999; **30**: 316–24.
23. Lerat H, Honda M, Beard MR, *et al.* Steatosis and liver cancer in transgenic mice expressing the structural and nonstructural proteins of hepatitis C virus. *Gastroenterology* 2002; **122**: 352–65.
24. Yagi K. A simple fluorometric assay for lipoperoxide in blood plasma. *Biochem Med* 1976; **15**: 212–6.
25. Healy LN, Pluta LJ, Recio L. Expression and distribution of cytochrome P450 2E1 in B6C3F1 mouse liver and testes. *Chem Biol Interact* 1999; **121**: 199–207.
26. Bradford MM. A rapid and sensitive method for the quantitation of microgram quantities of protein utilizing the principle of protein-dye binding. *Anal Biochem* 1976; **72**: 248–54.
27. Recknagel RO, Glende EA Jr, Dolak JA, Waller RL. Mechanisms of carbon tetrachloride toxicity. *Pharmacol Ther* 1989; **43**: 139–54.
28. Yan N, Meister A. Amino acid sequence of rat kidney gamma-glutamylcysteine synthetase. *J Biol Chem* 1990; **265**: 1588–93.
29. Gipp JJ, Bailey HH, Mulcahy RT. Cloning and sequencing of the cdna for the light subunit of human liver gamma-glutamylcysteine synthetase and relative mrna levels for heavy and light subunits in human normal tissues. *Biochem Biophys Res Commun* 1995; **206**: 584–9.
30. Poynard T, Bedossa P, Opolon P. Natural history of liver fibrosis progression in patients with chronic hepatitis C. The OBSVIRC, METAVIR, CLINIVIR, and DOSVIRC goups. *Lancet* 1997; **349**: 825–32.
31. Kato J, Kobune M, Nakamura T, *et al.* Normalization of elevated hepatic 8-hydroxy-2′-deoxyguanosine levels in chronic hepatitis C patients by phlebotomy and low iron diet. *Cancer Res* 2001; **61**: 8697–702.
32. Murakami C, Hino K, Korenaga M, *et al.* Factors predicting progression to cirrhosis and hepatocellular carcinoma in patients with transfusion-associated hepatitis C virus infection. *J Clin Gastroenterol* 1999; **28**: 148–52.
33. Weber LW, Boll M, Stampfl A. Hepatotoxicity and mechanism of action of haloalkanes: carbon tetrachloride as a toxicological model. *Crit Rev Toxicol* 2003; **33**: 105–36.
34. Jeong HG, You HJ, Park SJ, *et al.* Hepatoprotective effects of 18beta-glycyrrhetinic acid on carbon tetrachloride-induced liver injury: inhibition of cytochrome P450 2E1 expression. *Pharmacol Res* 2002; **46**: 221–7.
35. Wang L, Potter JJ, Rennie-Tankersley L, Novitskiy G, Sipes J, Mezey E. Effects of retinoic acid on the development of liver fibrosis produced by carbon tetrachloride in mice. *Biochim Biophys Acta* 2007; **1772**: 66–71.
36. Lopez-Diazguerrero NE, Luna-Lopez A, Gutierrez-Ruiz MC, Zentella A, Konigsberg M. Susceptibility of DNA to oxidative stressors in young and aging mice. *Life Sci* 2005; **77**: 2840–54.
37. Tomasi A, Albano E, Banni S, *et al.* Free-radical metabolism of carbon tetrachloride in rat liver mitochondria. A study of the mechanism of activaion. *Biochem J* 1987; **246**: 313–7.
38. Lu SC. Regulation of hepatic glutathione synthesis: current concepts and controversies. *FASEB J* 1999; **13**: 1169–83.

GASTROENTEROLOGY 2008;134:226–238

BASIC-LIVER, PANCREAS, AND BILIARY TRACT

Hepatitis C Virus–Induced Reactive Oxygen Species Raise Hepatic Iron Level in Mice by Reducing Hepcidin Transcription

SOHJI NISHINA,* KEISUKE HINO,‡ MASAAKI KORENAGA,* CHIARA VECCHI,§ ANTONELLO PIETRANGELO,§ YOICHI MIZUKAMI,‖ TAKAKAZU FURUTANI,* AYA SAKAI,‡ MICHIARI OKUDA,* ISAO HIDAKA,* KIWAMU OKITA,¶ and ISAO SAKAIDA*

*Departments of Gastroenterology and Hepatology and ‡Basic Laboratory Sciences and ‖Center for Gene Research, Yamaguchi University Graduate School of Medicine, Yamaguchi, Japan; ¶Department of Gastroenterology and Hepatology, Shimonoseki Kohsei Hospital, Yamaguchi, Japan; and §Center for Hemochromatosis, Department of Internal Medicine, University of Modena and Reggio Emilia, Modena, Italy

See editorial on page 348.

Background & Aims: **Despite abundant clinical evidence, the mechanisms by which hepatic iron overload develops in patients with hepatitis C virus (HCV)-associated chronic liver disease remain unknown. The aim of this study was to investigate how hepatic iron overload develops in the presence of HCV proteins.** ***Methods:*** **Male transgenic mice expressing the HCV polyprotein and nontransgenic control mice (C57BL/6) were assessed for iron concentrations in the liver, spleen, and serum and iron regulatory molecules in vivo and ex vivo.** ***Results:*** **Transgenic mice had increased hepatic and serum iron concentrations, decreased splenic iron concentration, and lower hepcidin expression in the liver accompanied by higher expression of ferroportin in the duodenum, spleen, and liver. In response to hepatocellular iron excess, transferrin receptor 1 expression decreased and ferritin expression increased in the transgenic liver. Transgenic mice showed no inflammation in the liver but preserved the ability to induce hepcidin in response to proinflammatory cytokines induced by lipopolysaccharide. Hepcidin promoter activity and the DNA binding activity of CCAAT/enhancer-binding protein α (C/EBP) were down-regulated concomitant with increased expression of C/EBP homology protein, an inhibitor of C/EBP DNA binding activity, and with increased levels of reactive oxygen species in transgenic mice at the ages of 8 and 14 months.** ***Conclusions:*** **HCV-induced reactive oxygen species may down-regulate hepcidin transcription through inhibition of C/EBPα DNA binding activity by C/EBP homology protein, which in turn leads to increased duodenal iron transport and macrophage iron release, causing hepatic iron accumulation.**

Hepatic iron overload is one of the pathophysiologic features of hepatitis C virus (HCV)-associated chronic liver disease,[1] even though the level of hepatic iron content is not extremely high.[2] Excess divalent iron can be highly toxic, mainly via the Fenton reaction producing hydroxyl radicals.[3] This is particularly relevant for chronic hepatitis C, in which oxidative stress has been proposed as a major mechanism of liver injury.[4] Oxidative stress and increased iron levels strongly favor DNA damage, genetic instability, and tumorigenesis. Indeed, we have reported that even modest iron supplementation induces hepatocellular carcinoma (HCC) in transgenic mice expressing the HCV polyprotein.[5] Kato et al reported that phlebotomy lowered the risk of progression to HCC,[6] which showed the critical role of iron in the development of HCC in patients with chronic hepatitis C. Thus, there is a critical interaction between HCV proteins and hepatic iron overload in the development of HCV-related HCC. However, the mechanism underlying hepatic iron overload in chronic hepatitis C remains elusive. Chronic inflammation produces proinflammatory cytokines that are involved in iron homeostasis such as tumor necrosis factor (TNF)-α, interleukin (IL)-1β, and IL-6.[7] Because the transgenic mice we have reported[5] do not show any inflammation in the liver, this animal model is suitable for investigating if the expression of HCV protein in the absence of inflammation affects iron metabolism.

Abbreviations used in this paper: C/EBP, CCAAT/enhancer-binding protein; CHOP, C/EBP homology protein; DMT1, divalent metal transporter 1; IL, interleukin; LPS, lipopolysaccharide; ROS, reactive oxygen species; RT-PCR, reverse-transcription polymerase chain reaction; TfR, transferrin receptor; TNF, tumor necrosis factor.

0016-5085/08/$34.00
doi:10.1053/j.gastro.2007.10.011

Table 1. Primers of the Genes Coding Hepcidin, Inflammatory Cytokines, and β-Actin

Gene	Sense	Antisense
Hepcidin	TCCTGCTTCTCCTCCTTGCC[1]	GTCTGCCCTGCTTTCTTCCC[1]
TNF-α	AAGCCTGTAGCCCACGTCGTA[2]	GGCACCACTAGTTGGTTGTCTTTG[2]
IL-1β	TCCAGGATGAGGACATGAGCAC[3]	GAACGTCACACACCAGCAGGTTA[3]
IL-6	CCACTTCACAAGTCGGAGGCTTA[4]	GCAAGTGCATCATCGTTGTTCATAC[4]
β-actin	TGACAGGATGCAGAAGGAGA[5]	GCTGGAAGGTGGACAGTGAG[5]

NOTE. The hepcidin primers are specific for both Hamp1 and Hamp2. GenBank accession numbers are NM_032541 for 1, NM_013693 for 2, NM_008361 for 3, NM_031168 for 4, and NM_007393 for 5.

The aim of this study was to investigate how hepatic iron overload develops in transgenic mice expressing the HCV polyprotein. In the present study, we report that HCV protein-induced reactive oxygen species (ROS) raise hepatic iron level by reducing transcription of hepcidin, a negative regulator of iron release, into the systemic circulation.[8]

Materials and Methods

Animals

The transgene pAlbSVPA-HCV, containing the full-length polyprotein-coding region, under the control of the murine albumin promoter/enhancer was described in detail.[9,10] HCV polyprotein has been shown to be processed into individual proteins in the liver and to be expressed at a biologically relevant level in which transcripts of RNA encoding the complete viral polyprotein are detectable only by reverse-transcription polymerase chain reaction (RT-PCR).[10] Of the 4 transgenic lineages with evidence of RNA transcription of the full-length HCV-N open reading frame (FL-N), the FL-N/35 lineage proved capable of breeding in large numbers. There was no inflammation in transgenic livers.[10] Male FL-N/35 transgenic mice and age-matched C57BL/6 mice were fed a normal rodent diet including carbonyl iron (45-mg/kg diet), bred, maintained, and killed by intraperitoneal injection of 10% pentobarbital sodium preceded by 12-hour fasting according to the criteria outlined in the Guide for the Care and Use of Laboratory Animals.

Histopathologic Procedures

Iron in liver sections was detected by Perls' Prussian blue staining. Ferric iron in the liver sections was histochemically examined using an Iron (II)/Iron (III) Detection kit (Stressgen, Victoria, Canada) with some modification.

Iron Concentrations in Liver, Spleen, and Serum

Iron concentrations in the liver and spleen were measured by atomic absorption spectrometry (Z-6100; Hitachi, Tokyo, Japan), as described previously,[5] and expressed as micrograms Fe per gram of tissue (wet weight). Serum iron concentrations were examined by a colorimetric method and measured with a Quick Auto Neo Fe (Synotest, Tokyo, Japan) according to the manufacturer's instructions.

RNA Isolation and Real-Time RT-PCR

One-step real-time RT-PCR was performed as described previously.[5] The primers amplifying the genes coding hepcidin and inflammatory cytokines are described in Table 1.

Hepatic Levels of Prohepcidin

The protein levels of prohepcidin, an 83–amino acid precursor with strong homology to hepcidin in its C-terminal region,[11] were quantified with a hepcidin prohormone enzyme-linked immunosorbent assay kit (DRG Instruments GmbH, Marburg, Germany) according to the manufacturer's instructions.

Immunohistochemical Detection of Ferroportin

Liver, spleen, and duodenum sections were incubated with a 1:200 dilution of a rabbit polyclonal anti-mouse ferroportin 1 antibody (Alpha Diagnostic International, San Antonio, TX) at 4°C overnight. Following incubation with avidin-conjugated peroxidase (Vecstatin Elite ABC; Vector Laboratories, Burlingame, CA), sections were developed in 3,3'-diaminobenzidine tetrahydrochloride (Sigma Chemical Co, St Louis, MO).

In Situ Detection of ROS

In the presence of ROS, dihydroethidium (Invitrogen Corp, Carlsbad, CA) is oxidized to ethidium bromide and stains nuclei bright red by intercalating with the DNA.[12] Fresh cross sections (10 μm) of unfixed, frozen liver tissues were immediately incubated with 5 μmol/L dihydroethidium at 37°C for 15 minutes in a humidified chamber, subsequently washed twice with ice-cold phosphate-buffered saline, and cover slipped. Fluorescence intensity was quantified using NIH image analysis software for 3 randomly selected areas of digital images in each mouse.

Immunoblotting

Lysates of liver, spleen, and duodenum were separated by sodium dodecyl sulfate/polyacrylamide gel electrophoresis. The proteins were transferred to polyvinylidene difluoride membranes (Millipore, Bedford, MA), blocked overnight at 4°C with 5% skim milk and 0.1% Tween 20 in Tris-buffered saline, and subsequently incubated for 1 hour at room temperature with an anti-mouse ferroportin 1

antibody (Alpha Diagnostic International), anti-mouse divalent metal transporter 1 (DMT1) antibody (Santa Cruz Biotechnology Inc, Santa Cruz, CA), anti-human ferritin antibody (Dako, Glostrup, Denmark), anti-human transferrin receptor (TfR) 1 antibody (Zymed Laboratories, San Francisco, CA), anti-rat CCAAT/enhancer-binding protein α (C/EBPα) antibody (Santa Cruz Biotechnology Inc), or antibacterially expressed, mouse C/EBP homology protein (CHOP) fusion protein antibody (Abcam, Cambridge, England).

Injection of Lipopolysaccharide

Lipopolysaccharide (LPS, 1 μg/g body wt, *Escherichia coli* 0111:B4; Sigma Chemical Co) or an equivalent volume of phosphate-buffered saline was injected intraperitoneally, and liver samples were isolated for RNA preparation 6 hours after injection.

Isolation and Culture of Primary Hepatocytes

Hepatocytes were isolated from FL-N/35 transgenic mice and nontransgenic mice by a 2-step collagenase perfusion procedure. They were then seeded in Williams' medium E (Invitrogen Corp) and supplemented with 10% fetal calf serum, penicillin (100 u/mL)-streptomycin (100 μg/mL) (Invitrogen Corp), and 100 nmol/L insulin. Four hours later, the medium was renewed with the same medium.

Cloning of Mouse Hepcidin Promoter and Construction of Reporter Vectors

The murine hepcidin promoter region was cloned by PCR using mouse DNA as a template and specific hepcidin primers: mHAMPpr_789 fw 5'- GCGCTCGAGGAATACATCGTCAAGCCAGAC-3' mHAMPpr_318_fw 5'-TTCCTCGAGTCACCAATCCAATCACTGTTTAGG-3' mHAMPpr_124_fw 5'-GCCCTCGAGGCGCCACTATTTTCTTGGAA-3' and mHAMPpr_rev 5'-GCGAAGCTTGTGTGGTGGCTGTCTAGGAGC-3' (the incorporated *Xho*I and *Hin*dIII sites are underlined). PCR products were then purified, digested with *Xho*I/*Hin*dIII, and subcloned in the pGL3-Luc (Promega, Madison, WI) plasmid upstream of the firefly luciferase gene.

Cell Transfection and Luciferase Assay

Primary hepatocytes obtained from 4 mice in each group were transiently transfected with pGL3 Basic vector (negative control), pGL3-CMV vector (positive control), or reporter vectors containing the mouse hepcidin promoter region (pGL3_mHAMP124 [−110/+14], pGL3_mHAMP318 [−304/+14], or pGL3_mHAMP789 [−775/+14]) by using TransFectin Lipid Reagent (Bio-Rad Laboratories Inc, Hercules, CA) 24 hours after cell seeding. The pSV-β-galactosidase control vector encoding β-galactosidase (Promega) used as a cotransfectant served as the control for transfection efficiency. Cellular extracts were analyzed for luciferase activity with a Luciferase assay system (Promega) 48 hours after transfection. β-Galactosidase enzyme assay was performed using the β-galactosidase Enzyme Assay System (Promega). Each assay was performed in duplicate.

Electrophoretic Mobility Shift Assay

Nuclear extracts were obtained using a Nuclear Extraction Kit (Panomics, Redwood, CA), following the manufacturer's instructions. Five micrograms of the nuclear extracts was incubated for 30 minutes at room temperature with horseradish peroxidase–labeled oligonucleotide probe 5'-CATGGATGGTATTGAGAAATCTG-3' (C/EBP binding site is underlined)[12] using an EMSA Gel-Shift Kit (Panomics) according to the manufacturer's instructions.

Quantification of C/EBP Activation

C/EBPα and C/EBPβ activation was quantified using a Trans AM C/EBP α/β kit (Active Motif, Carlsbad, CA), following the manufacturer's instructions. Briefly, 5 μg of nuclear extract was added to a well to which an oligonucleotide encoding the C/EBP consensus binding site had been immobilized. C/EBPα and C/EBPβ contained in nuclear extract were detected by an antibody directed against either C/EBPα or C/EBPβ.

Statistical Analysis

Quantitative values are expressed as mean ± SD. Two groups at each time point were compared by the Student *t* test. Two groups among multiple groups were compared by the rank-based, Kruskal–Wallis analysis of variance test followed by Scheffe's test. A *P* value of less than .05 was considered significant.

Results

Increased Iron Levels in Liver and Serum and Decreased Iron Level in Spleen

FL-N/35 transgenic mice fed a normal rodent diet had greater hepatic iron contents at the ages of 8 ($P < .05$) and 14 months ($P < .05$) than nontransgenic mice (Figure 1*A*). Serum iron levels were also significantly greater in FL-N/35 transgenic mice at the ages of 8 ($P < .05$) and 14 months ($P < .01$) (Figure 1*B*). Transferrin saturation was significantly greater in FL-N/35 transgenic mice than in nontransgenic mice at the ages of 8 (55.1% ± 12.1% vs 40.2% ± 12.0%; $P < .05$) and 14 months (47.3 ± 8.6 vs 35.8 ± 5.6; $P < .05$). In contrast, splenic iron content was significantly lower in FL-N/35 transgenic mice at the ages of 8 ($P < .05$) and 14 months ($P < .01$) (Figure 1*C*). Thus, it appeared that hepatic iron accumulation in FL-N/35 transgenic mice likely resulted from increased intestinal iron absorption and/or increased iron release from macrophages.

As shown in Figure 1*D*, FL-N/35 transgenic mice had histologically mild but clear iron accumulation in the liver as compared with nontransgenic mice (Figure 1*D*, I and II). Immunohistochemical analysis and high

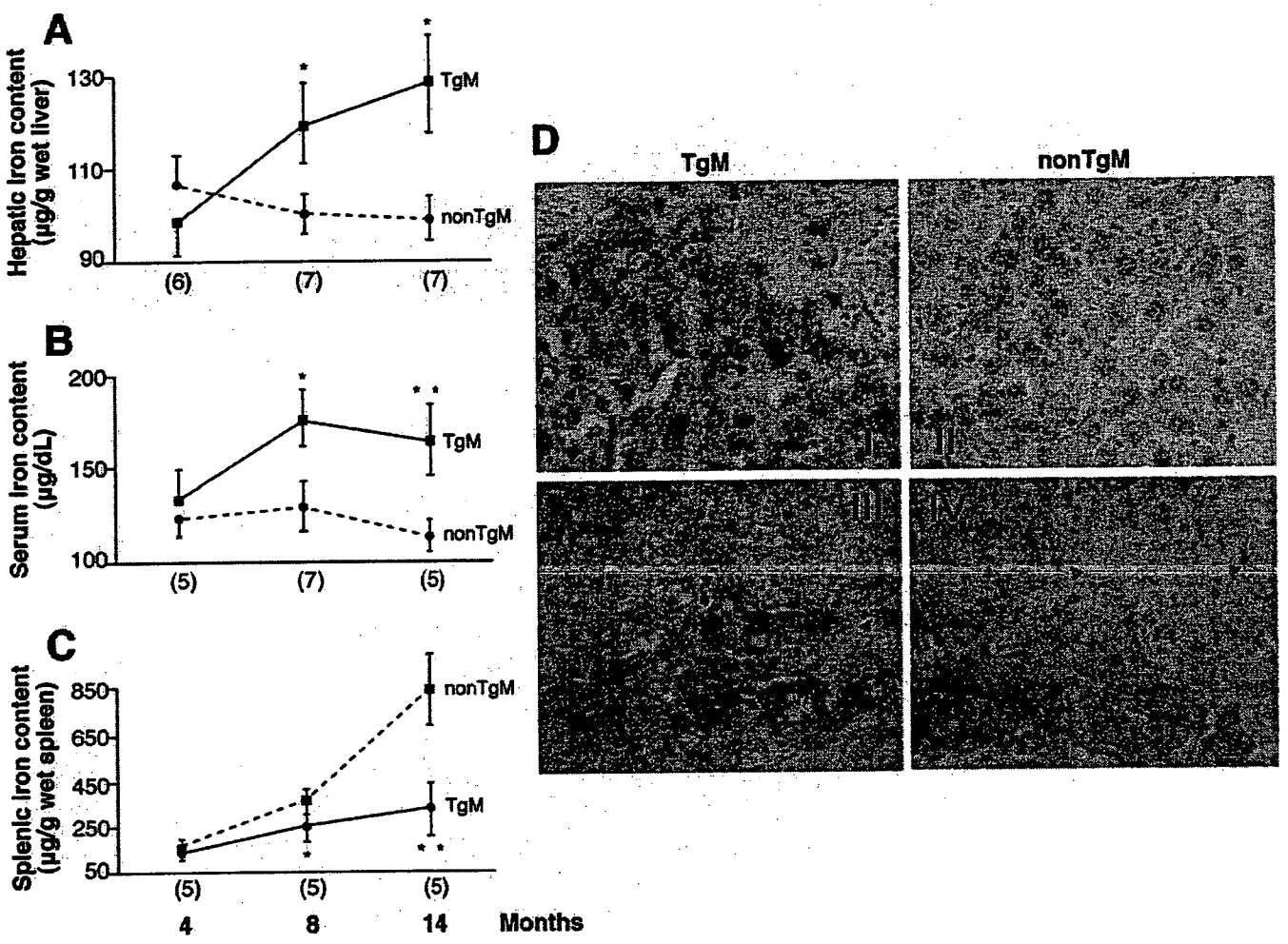

Figure 1. Iron concentrations in the liver, serum, and spleen and iron localization in the liver. (*A*) Hepatic and (*C*) splenic iron concentrations were measured by atomic absorption spectrometry in mice at the ages of 4, 8, and 14 months. (*B*) Serum iron levels were measured using a colorimetric method. $^{*}P < .05$, $^{**}P < .01$ versus same-age nontransgenic mice (nonTgM). The numbers in parentheses represent the number of animals examined in each group. (*D*) Iron in liver sections was examined by Perls' Prussian blue staining (I and II: original magnification 400×) and by immunohistochemical method in TgM and nonTgM (III and IV: original magnification 1000×) at the age of 8 months. *Arrows* indicate the sinusoidal lining cells. TgM, FL-N/35 transgenic mice.

magnification made it possible to differentiate iron localization in sinusoidal lining cells from that in hepatocytes. Ferric iron was localized in both hepatocytes and sinusoidal lining cells but was predominantly present in hepatocytes in FL-N/35 transgenic mice (Figure 1*D*, III and IV).

Hepcidin Levels in Liver

Because there is no known regulatory mechanism for iron excretion, systemic iron homeostasis is maintained by tight regulation of intestinal iron absorption and macrophage iron release.[13] Although the mechanism for this remains to be fully elucidated, hepcidin, a peptide hormone secreted by the liver,[8] seems to have a key role. Hepatic hepcidin messenger RNA (mRNA) levels were significantly lower in FL-N/35 transgenic mice at the ages of 8 ($P < .05$) and 14 months ($P < .01$) (Figure 2*A*). Similarly, protein levels of prohepcidin were significantly lower in FL-N/35 transgenic mice at the ages of 8 ($P < .05$) and 14 months ($P < .01$) (Figure 2*B*). These results suggested that hepatic iron accumulation was closely associated with decreased hepcidin expression in the transgenic mice.

Expression of Ferroportin in Duodenum, Spleen, and Liver

Hepcidin binds to the iron exporter ferroportin, which results in internalization and degradation of ferroportin.[14] Diminished hepcidin expression, therefore, is expected to lead to stabilization of ferroportin, with increased mobilization of iron from macrophages and, presumably, increased intestinal uptake as well. As shown in Figure 3*A*, several clusters of cells stained positively for ferroportin were present in the duodenum, spleen, and liver in FL-N/35 transgenic mice, whereas such clusters were nearly absent in all 5 nontransgenic mice at the age

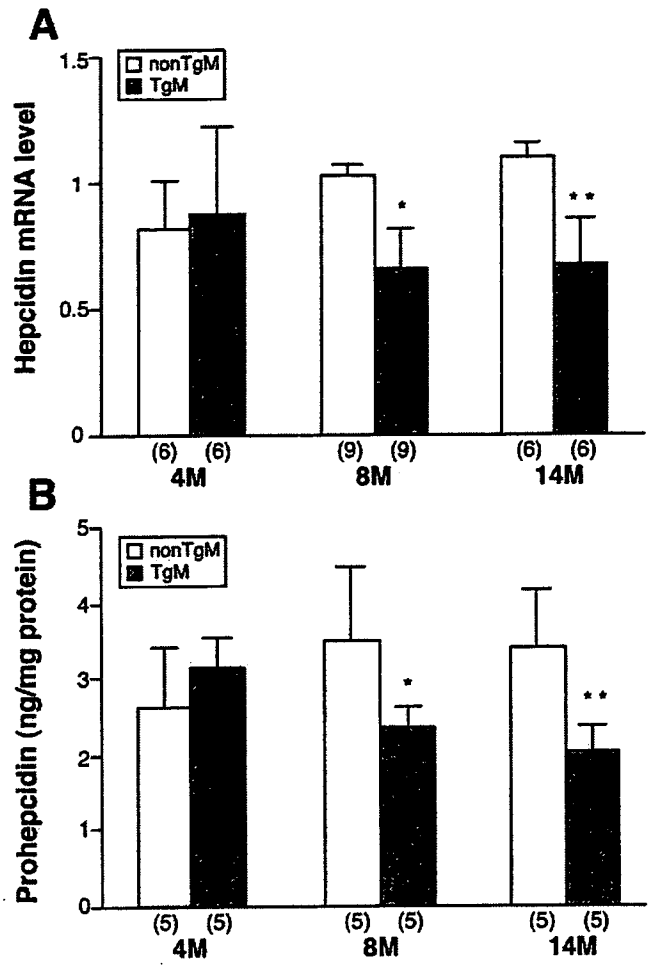

Figure 2. Hepatic levels of hepcidin mRNA and prohepcidin. The expression levels of (*A*) hepcidin mRNA and (*B*) prohepcidin were measured by real-time RT-PCR and enzyme-linked immunosorbent assay, respectively. The relative quantities of hepcidin mRNA in the liver were normalized to β-actin mRNA. The relative protein levels of prohepcidin were normalized by protein concentrations and expressed as nanogram per milligram protein. *$P < .05$ (8 months) and **$P < .01$ (14 months) versus same-age nontransgenic mice (nonTgM). The numbers in parentheses represent the number of animals examined in each group. TgM, FL-N/35 transgenic mice.

of 14 months. Hepatic expression of ferroportin was found in both hepatocytes and sinusoidal lining cells, probably Kupffer cells, with predominant localization in sinusoidal lining cells (Figure 3*A*). The expression of ferroportin in the duodenum, spleen, and liver was greater in FL-N/35 transgenic mice at the age of 8 and/or 14 months (Figure 3*B*). Hepatic expression of ferroportin did not appear to increase to the same degree as expression in the duodenum and spleen (Figure 3*B*).

Expression of DMT1 in Duodenum and Liver

DMT1 is an apical iron transporter in the duodenum and may participate in the uptake of non-transferrin-bound iron by hepatocytes.[15] The expression of DMT1 in the duodenum and liver was similar in FL-N/35 transgenic mice and nontransgenic mice (Figure 4) at the ages of 4, 8, and 14 months. Because transferrin saturation was approximately 50% at the ages of 8 and 14 months in FL-N/35 transgenic mice, it is unlikely that non-transferrin-bound iron contributed significantly to circulating iron. Our results suggested that an increase in DMT1 protein in either duodenum or liver was not required for hepatic iron accumulation in FL-N/35 transgenic mice.

Expression of Ferritin and TfR1 in Liver

Intracellular iron excess inhibits the binding of iron regulatory proteins to iron-responsive elements in the 5′-untranslated region of ferritin mRNA and 3′-untranslated region of TfR1 mRNA, which allows the translation of ferritin mRNA and decreases the stability of TfR1 mRNA.[16] Ferritin consists of H subunits and L subunits that assemble to form a shell of 24 subunits with a cavity capable of storing up to 4500 Fe atoms as hydrous ferric oxide polymers.[17] As shown in Figure 5*A*, the expression of L subunits of ferritin was significantly greater in FL-N/35 transgenic mice than in nontransgenic mice at the ages of 8 ($P < .01$) and 14 months ($P < .05$). Although H subunits could not be detected, this was consistent with the results of experimentally iron-overloaded C57BL/6 mice.[18] H subunits of ferritin in the liver may be difficult to detect with the anti-ferritin antibody used in both studies.

We next measured the expression of TfR1 in the liver to assess if it showed appropriate iron-dependent regulation. As shown in Figure 5*B*, the expression of TfR1 protein was significantly lower in FL-N/35 transgenic mice at the ages of 8 and 14 months ($P < .01$).

Hepcidin Expression in Response to Inflammation

Hepcidin expression is enhanced by iron overload and inflammation.[7,11] We next examined if the present animal model preserved the ability to induce hepcidin in response to inflammation. Induction of acute inflammation by LPS injection led to significant up-regulation of TNF-α, IL-1β, and IL-6 in the liver in both FL-N/35 transgenic mice and nontransgenic mice. With up-regulation of inflammatory cytokines, hepatic hepcidin expression was significantly increased by LPS injection in both FL-N/35 transgenic mice and nontransgenic mice (Figure 5*C*).

Promoter Activity of Hepcidin

To study the effects of HCV proteins on the transcriptional regulation of hepcidin, reporter gene assays were performed for primary mouse hepatocytes. Two reporter vectors, pGL3_mHAMP318 and pGL3_mHAMP789, exhibited significantly lower luciferase activity in FL-N/35 transgenic hepatocytes than in nontransgenic hepatocytes at the ages of 8 and 14 months ($P < .05$) (Figure 6*B*). Thus, the transcriptional activity of hepcidin was